Journal of Applied Electrochemistry **33**: 431–441, 2003.

Influence of agarose on the electrochemical behaviour of the silver and platinum aqueous acid electrolyte interface

M.A. PASQUALE, S.L. MARCHIANO, A.E. BOLZÁN and A.J. ARVIA*
Instituto de Investigaciones Físicoquimicas Teóricas y Aplicadas (INIFTA), Consejo Nacional de Investigaciones Científicas y Técnicas, Universidad Nacional de La Plata, Sucursal 4, Casilla de Correo 16, (1900) La Plata, Argentina
*(*author for correspondence, fax: +54 221 4254642, e-mail: ajarvia@inifta.unlp.edu.ar)*

Received 30 July 2002; accepted in revised form 13 December 2002

Key words: agarose, electrooxidation, gels, platinum, silver, sols

Abstract

The influence of agarose on the electrochemical behaviour of the interfaces silver/aqueous agarose + 0.014 M silver sulfate + 0.5 M sodium sulfate + 0.01 M sulfuric acid and platinum/aqueous agarose + 0.5 M sulfuric acid, at 298 K, was studied. Freshly prepared and aged agarose-containing solutions in the range of agarose concentration $0.01 \leqslant c_{aga} \leqslant 0.5\%$ w/v were used. Viscosity, open circuit potential, solid sample infrared spectra and conventional voltammetric measurements were performed. The electrooxidation of adsorbates produced from both the homogeneous and heterogeneous decomposition of agarose-containing solutions on platinum was investigated. Results are discussed in terms of the structure and interactions of agarose molecules in sols and gels. The electrooxidation of adsorbed residues can be explained within the complex reaction pathway for the electrooxidation of saccharides previously discussed in the literature.

1. Introduction

The kinetics of electrochemical processes involving high values of exchange currant density (j_0) and low cell resistance are usually controlled by ionic mass transfer processes, that is, diffusion, migration and convection. The influence of each of these processes on the electrochemical reactions can be determined by an appropriate choice of solution composition. Thus, migration is suppressed by adding an excess of supporting electrolyte to the working solution, and free convection in stagnant solutions can be prevented by adding a gel-forming constituent to the solution. For low additive concentrations, this solution generally behaves as a non-newtonian sol, and when a threshold concentration of additive is exceeded a gel phase is formed. The kinetics of the electrochemical process in the gelled solution are then pure diffusion controlled [1–6]. In any case, the presence of an additive implies the appearance of new molecular interactions in the system that should be reflected in the kinetics and mechanism of the reaction. For this purpose, additives such as carboxymethyl-cellulose [1] and agarose [2–5] in aqueous electrolytes that are easy to manipulate, sufficiently stable at room temperature and form gels for concentrations above a certain critical concentration, are used in a number of technical processes.

Agarose sols formed in concentrations as low as 0.04% w/v have been used to determine the influence of viscosity on the kinetics of heterogeneous processes, as these sols are able to decrease buoyancy driven natural convection. As the agarose concentration is further increased, the apparent viscosity of the solution also increases and the contribution of free convection to the process gradually diminishes [7]. Thus, by changing the concentration of agarose it is possible to adjust the rheological properties [1–7]. Recently, aqueous agarose-containing solutions have been used to study the influence of diffusion and free convection on the growth modes of silver electrodeposits [3–8] using both 3D [5] and quasi-2D electrochemical cells [2, 8]. In this work, however, it was not possible to determine whether agarose, as well as its influence on the viscosity of the solution in the form of agarose sols and gels, might produce additional effects from agarose itself or its decomposition products at the metal–solution interface.

Agarose is an alternating polysaccharide copolymer of algal origin, its backbone containing $(1 \rightarrow 4)$ and $(1 \rightarrow 3)$ linked 3,6-anhydro-α-L-galactose (Figure l(a)) [6, 9, 10]. The 4-linked residues give rise to an extended ribbon, whereas the 3-linked units generate a hollow helix [9, 10]. A large part of the agar backbone can be substituted with neutral and charged groups. X-ray

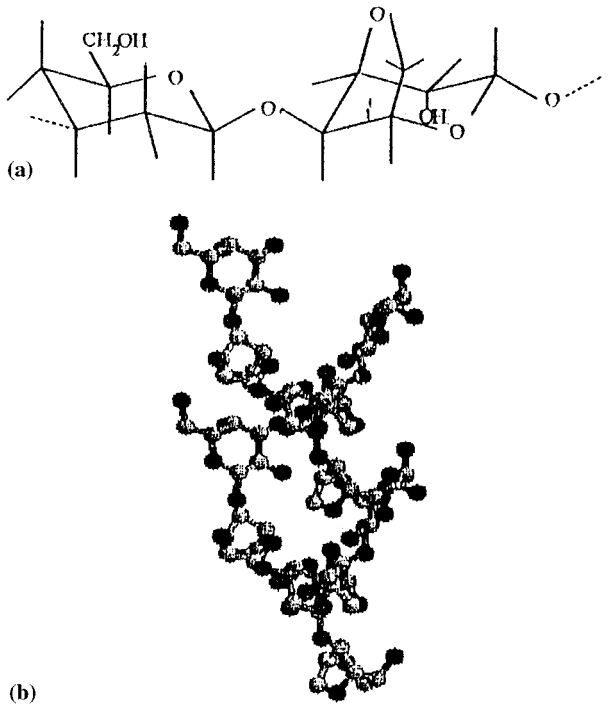

Fig. 1. (a) Primary structure of agarose: [→3)-β-D-Galp-(1→4)-3,6-anhydro-α-L-Galp-(1→] (repeating unit). (b) Hollow helix structure of agarose from [7].

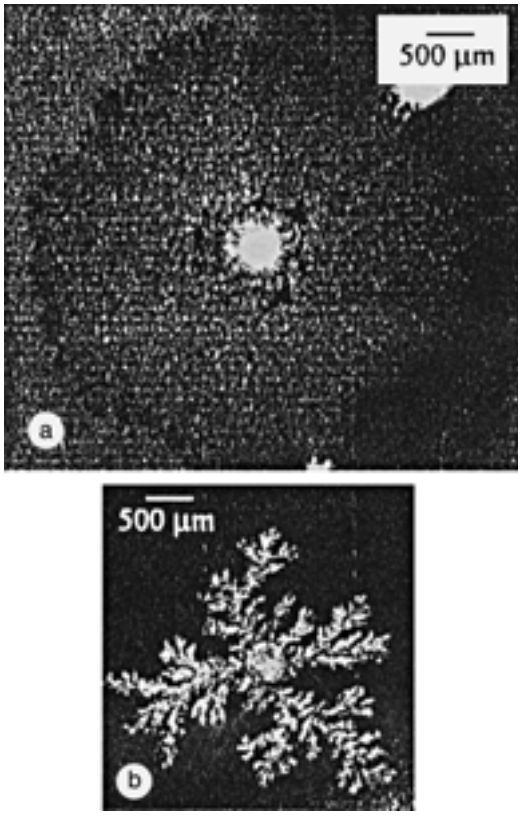

Fig. 2. Typical silver growth patterns produced by electrodeposition from a quasi-2D electrochemical cell using different plating solutions for ΔE (cathode-to-anode) = −0.518 V at 298 K. (a) Aqueous 0.014 M silver sulfate + 0.01 sulfuric acid + 0.5 M sodium sulfate, electrolysis time 400 s. (b) Gel prepared from the same solution with the addition of 0.5% w/v agarose, electrolysis time 727 s.

diffraction supports a double helix model consisting of parallel threefold chains with a left-handed sense and a pitch of 1.90 nm [9] (Figure 1(b)). The double helix structure can persist under hydrated conditions in solutions and gels. Consequently, changes in the nature and degree of substitution produce a change in the stability of the ordered structure and in its aggregation state. The formation of gels involves the association of chains through double helices to develop a three-dimensional network [6, 9].

This work reports some electrochemical properties and the stability of different aqueous agarose-containing electrolytes employed to investigate the influence of viscosity on the growth mode of silver electrodeposits on polycrystalline platinum substrates, particularly under gelling to achieve pure diffusion [8]. The influence of agarose on the growth patterns of silver resulting from silver deposition is illustrated in Figure 2. Under similar conditions, in the absence of agarose the growth pattern results in a dense branched structure with a fractal surface (Figure 2(a)), whereas in agarose-containing solution an open branched pattern that behaves as a surface and mass fractal is obtained (Figure 2(b))[5, 8].

2. Experimental details

Different solutions consisting of either aqueous 0.02% w/v agarose, aqueous agarose-containing 0.5 M sulfuric acid or aqueous agarose-containing 0.014 M silver sulfate + 0.5 M sodium sulfate + 0.01 M sulfuric acid, with an agarose content in the range $0 \leqslant c_{aga} \leqslant 0.8\%$ w/v, either freshly prepared or standing for different times, were used [8]. Solutions were prepared from pure agarose (Merck, sulfur/carbon elemental ratio less than 0.4% w/v), analytical reagent grade chemicals (Merck) and Milli-Q* water. All runs were made at 298 K. Polycrystalline platinum wires (0.07 cm dia., 99.99% purity, Goodfellow, England) subjected to conventional cleaning procedures were used as working electrodes. Potentials in the text are given against the standard hydrogen electrode (SHE) scale.

2.1. *Electrochemical measurements*

The rest potential under open circuit (E_{rest}) of polycrystalline platinum in aqueous agarose 0.02% w/v + 0.5 M sulfuric acid, and silver in aqueous agarose 0.10% w/v + 0.014 M silver sulfate + 0.5 M sodium sulfate + 0.01 M sulfuric acid was measured for both freshly prepared and standing solutions. The latter were stored for as long as two weeks.

The voltammetric underpotential electrodeposition (upd)/anodic stripping of lead from aqueous 0.01 M lead perchlorate + 0.01 M perchloric acid + 0.5 M sodium perchlorate as test reaction, was run at $v = 0.01$ V s^{-1}, using a silver-coated platinum electrode prepared by coulostatic ($q_c = 40$ mC cm^{-2}) silver plat-

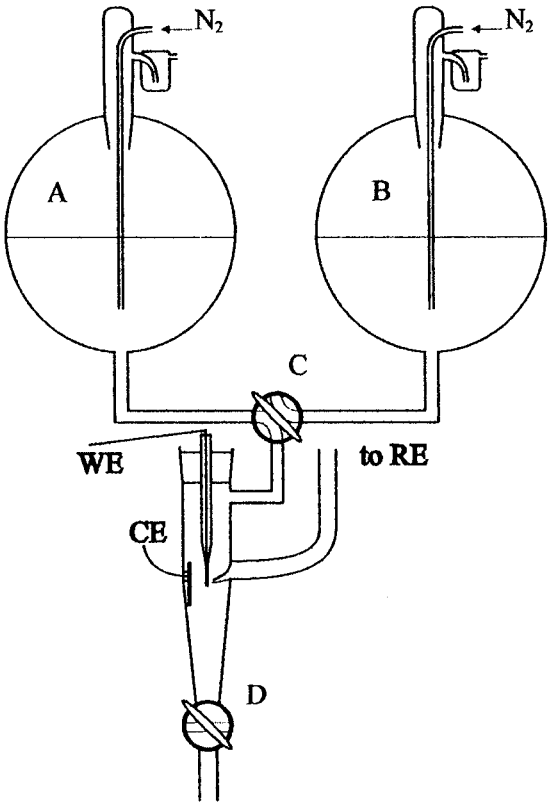

Fig. 3. Scheme of the flow electrochemical cell. Key: (A) and (B) solution reservoirs; (C) connecting stopcock; (D) drainage stopcock; (WE) working electrode; (CE) counter electrode; (RE) connection to the reference electrode.

ing from aqueous 5×10^{-5} M silver sulfate + 0.01 M perchloric acid + 0.5 M sodium perchlorate.

Voltammetry on platinum electrodes at 0.05 V s^{-1} was performed by running either single or repetitive triangular potential scans covering the range 0–1.4 V. Adsorption and electroadsorption runs were carried out at different constant potentials E_{ad} and times t_{ad}.

Additionally, electrochemical experiments on platinum were made using the flow cell technique following the procedure described previously [11, 12] (Figure 3). For this purpose, a potential step E_{ad} ($0.658\ V \geqslant E_{ad} \geqslant 0.080$ V) was applied to the working electrode, and simultaneously the current evolution was followed.

2.2. *Viscometry*

Viscosity data for plain aqueous agarose and aqueous agarose-containing electrolyte solutions, either freshly prepared or standing for several weeks, were obtained. The flow times were determined using an Ostwald viscometer. Data from these experiments combined with those from electrochemical measurements allowed us to establish the stability range of the working solutions.

2.3. *Infrared spectroscopy*

Infrared spectra of solid samples of agarose, and gelled agarose separated from aqueous agarose 0.10% w/v + 0.014 M silver sulfate + 0.5 M sodium sulfate + 0.01 M sulfuric sol, both in potassium bromide, were recorded using a Shimadzu infrared spectrophotometer (IR-435).

3. Results

3.1. *Change of rest potential*

The change in E_{rest}, can be related to the stability of the agarose-containing solutions. For a silver electrode immersed in aqueous 0.05% w/v agarose + 0.014 M silver sulphate + 0.5 M sodium sulfate + 0.01 M sulfuric acid, $E_{rest} = 0.669 \pm 0.025$ V. This value is close to the reversible electrode potential of the Ag/Ag^+ couple for $c_{Ag_2SO_4} = 0.014$ M at 298 K, E_{rev}/V vs SHE = 0.675, and it remained constant for at least two weeks. A different situation was found for platinum immersed in aqueous 0.1% w/v agarose + 0.5 M sulfuric acid (Figure 4). In this case, initially it was observed that $E_{rest} = 0.904$ V, a figure that, over five days, decreased steadily to the minimum value $E_{rest} = 0.694$ and, after the following three days, recovered slowly to $E_{rest} = 0.769$ V. For platinum, this change of E_{rest} is consistent with the corresponding change in the voltammograms, as described later. Both changes agree with the well known adsorption properties of platinum electrodes in the presence of organic substances [13].

3.2. *Voltammetric data of lead upd/anodic stripping on silver-plated platinum*

The aim of these experiments was to determine the extent of free silver surface after the working electrode has been immersed in aqueous agarose-containing solutions for a certain time. The presence of adsorbates from either agarose or products from agarose

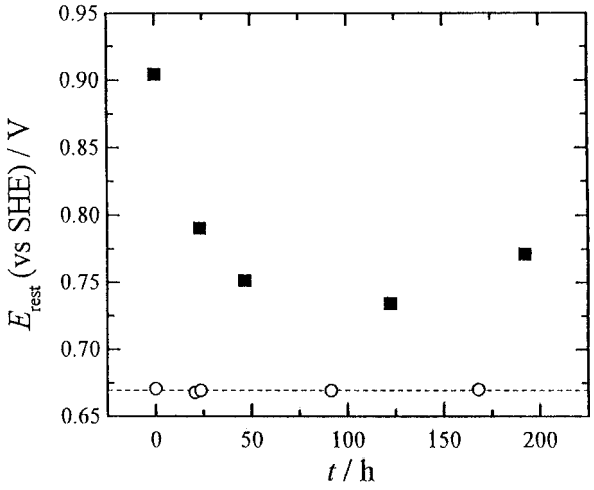

Fig. 4. Open circuit potential against time plot for aqueous 0.02% w/v agarose + 0.5 M sulfuric acid (■)+ 0.014 M silver sulfate + 0.5 M sodium sulfate + 0.01 M sulfuric acid (○). Nitrogen saturation; 298 K.

decomposition would produce either a decrease in the overall voltammetric charge due to partial blockage of the electrode surface or a distortion in the lead upd voltammogram due to change in the energy distribution of surface sites.

Each silver-plated electrode was rinsed with water and immersed, at open circuit, in freshly prepared aqueous 0.02% w/v agarose. Subsequently, the electrode was transferred to another cell containing aqueous 0.01 M lead perchlorate + 0.01 perchloric acid + 0.5 M sodium perchlorate, and then lead upd/anodic stripping cyclic voltammograms in the range $-0.155\ \text{V} \leqslant E \leqslant 0.245\ \text{V}$, at $v = 0.01\ \text{V s}^{-1}$ were run (Figure 5). For $c_{\text{aga}} \rightarrow 0$ and $t_{\text{ad}} \rightarrow 0$, these voltammograms exhibit a multiplicity of cathodic and anodic peaks resembling those already known for silver electrodes [14–19]. Otherwise, for $t_{\text{ad}} < 60$ min, only slight changes in the voltammetric features, as compared to those in the blank, are observed (Figure 5(b)), but for $t_{\text{ad}} > 1$ h, the sharp structure of the current peaks smears out. In all cases, however, the voltammetric cathodic and anodic charge density is almost the same, that is, $q_{\text{a}} = q_{\text{c}} = 0.47\ \text{mC cm}^{-2}$, irrespective of t_{ad}.

Results from these experiments indicate that for $t_{\text{ad}} < 60$ min, the surface blockage produced by the presence of agarose, if any, should be smaller than 5%. Agarose appeared to exert some influence on the energetics of silver electrocrystallization because of the shift in the peak potentials, as well as distortion of the current peaks in the lead upd/anodic stripping voltammograms. This is not surprising, since the presence of agarose produces changes in the growth mode of the silver deposits [2, 8, 19]. On the other hand, for $t_{\text{ad}} > 60$ min, the enhancement of these effects for agarose-containing solutions only, is consistent with the presence of products of lower molecular weight yielded by agarose standing decomposition that interfere to in the electrochemical process.

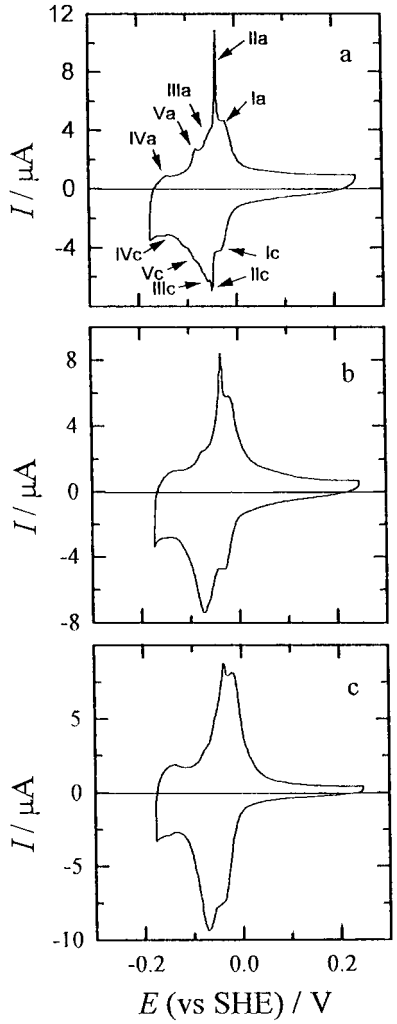

Fig. 5. Lead upd/anodic stripping voltammograms run at 0.001 V s^{-1} on silver-plated platinum electrodes immersed in aqueous 0.01 M lead perchlorate + 0.01 M perchloric acid + 0.5 M sodium perchlorate. 298 K. Apparent electrode area 0.159 cm^2. (a) Blank, (b) After immersion in aqueous 0.05% w/v agarose for $t_{\text{ad}} > 1$ h, and (c) for $t_{\text{ad}} > 4$ h. The fine voltammetric structure smears out as t_{ad} is increased, although the overall anodic and cathodic voltammetric charge remains almost the same.

3.3. *Agarose–platinum electrode interactions*

First, the initial voltammogram of platinum in aqueous 0.5 M sulfuric acid in the range 0–1.4 V was recorded. To determine adsorption phenomena involving either agarose or products from its decomposition, each electrode was first immersed in freshly prepared aqueous 0.02% w/v agarose + 0.5 M sulfuric acid by holding the applied potential in the range $0.0\ \text{V} \leqslant E_{\text{ad}} \leqslant 0.2\ \text{V}$ for a time in the range $0 \leqslant t_{\text{ad}} \leqslant 3600$ s. Immediately afterwards the electrode was rinsed with aqueous 0.5 M sulfuric acid to remove vestiges of the agarose-containing solutions, and holding the potential at $E_{\text{ad}} = 0.39$ V, it was immersed again in aqueous 0.5 M sulfuric acid to run a single triangular potential scan from 0.390 to 0 V, backwards to the anodic switching potential $E_{\text{a}} = 1.4$ V, and finally downwards to 0.390 V (Figure 6).

These voltammograms show a progressive decrease and a gradual distortion of current peaks related to hydrogen atom electrosorption occurring in the range 0–0.3 V. These effects increase with t_{ad}. Correspondingly, the positive potential scan in the range 0.75–1.4 V, that is, in the potential window where oxygen-containing surface species on platinum are formed, also show a gradual decrease in the anodic peak at 0.9 V (peak II), and the appearance of a new anodic peak at 1.175 V (peak III) that gradually decreases on potential cycling. Simultaneously, a slight decrease in the electroreduction charge of the oxygen-containing surface layer is observed, as if the formation of this layer would be delayed by the presence of agarose decomposition products remaining on the electrode surface after the electrooxidation scan (Figure 6). The possibility that the anodic peak III would result from a sulfur-containing layer produced at E_{rest} was discarded because we obtained a negative EDAX result on a platinum electrode that had been immersed for 4 h in the same agarose-containing

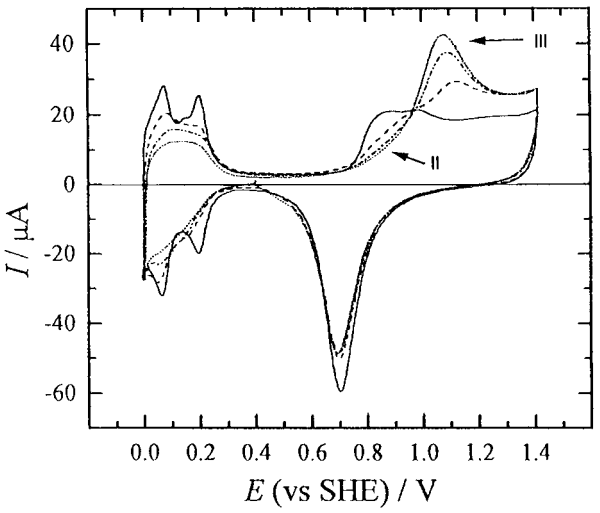

Fig. 6. Voltammograms obtained on polycrystalline platinum at 0.05 V s^{-1} after immersion of the electrode held at $E_{ad} = 0.20$ V in freshly prepared aqueous 0.02% w/v agarose + 0.5 M sulfuric acid for different t_{ad}. Dotted trace: $t_{ad} = 1$ h; dot-dashed trace: $t_{ad} = 20$ min; dashed trace: $t_{ad} = 5$ min. Full trace corresponds to the blank. Working electrode geometric area 0.159 cm^2 at 298 K.

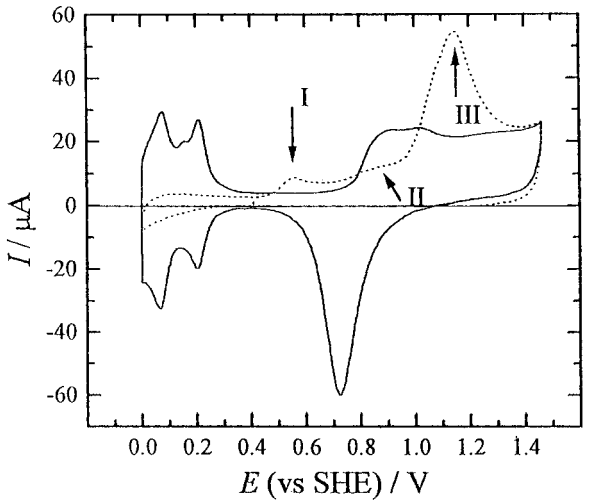

Fig. 7. Voltammograms obtained on polycrystalline platinum at 0.05 V s^{-1} after immersion of the electrode held at 0.44 V. Dashed trace: for $t_{ad} = 1$ h in 15 days standing aqueous 0.02% w/v agarose + 0.5 M sulfuric acid. Full trace corresponds to the blank. Working electrode geometric area 0.159 cm^2 at 298 K.

solution. Therefore, it is reasonable to relate peak III to the electrooxidation of agarose residues interacting with platinum.

The charge of peak III would comprise the electrooxidation of adsorbates from agarose that remained on the electrode after the potential scan from 0.5 to 0 V, and the competitive electrooxidation of water on the free platinum surface from 0.7 V upwards leading to the formation of the oxygen-containing layer on platinum. The charge associated with peak III, which is related to the electrooxidation of adsorbates from agarose, was evaluated for each t_{ad} by subtracting from the total electrooxidation charge the electroreduction charge of the oxygen-containing layer. The latter was determined from the area of the cathodic peak at 0.685 V.

The same type of experiment was made with aqueous 0.02% w/v agarose + 0.5 M sulfuric acid after standing for two weeks. These voltammograms (Figure 7) exhibit a remarkable decrease in the hydrogen atom electrosorption charge, the appearance of peak III and two small anodic peaks at 0.55 V (peak I) and 0.85 V (peak II). The latter also appeared as a little hump in the voltammograms of platinum in freshly prepared agarose-containing solutions.

Quantitative data related to adsorption phenomena on platinum in aqueous agarose-containing 0.5 M sulfuric acid at constant E_{ad} ($0 \text{ V} \leqslant E_{ad} \leqslant 0.658$ V) in the range from the hydrogen adatom fractional monolayer coverage up to the threshold potential of the oxygen-containing submonolayer formation were obtained. These data were expressed in terms of the percentage degree of surface coverage $\theta = (q_H^0 - q_H)100/q_H^0$, where q_H^0 and q_H are the electrooxidation charge density of hydrogen adatoms resulting from $c_{aga} = 0$, and $0.01; \leqslant c_{aga} \leqslant 0.08\%$ w/v, respectively. For $t_{ad} = 10$ min, and the ranges of E_{ad} and c_{aga} already mentioned, this results in $\theta = 25\%$ (Figure 8). Likewise, at constant E_{ad} in the range $0.0 \text{ V} \leqslant E_{ad} \leqslant 0.2$ V, and $c_{aga} = 0.02\%$ w/v, the influence of t_{ad} on θ was determined. Kinetic data resulting from freshly prepared agarose-containing solutions were used to estimate the rate of poisoning of platinum electrode by adsorbates, estimated from the rate of hydrogen atom electrosorption inhibition in the range $0.0 \text{ V} \leqslant E \leqslant 0.2$ V (Figure 9(a) and (b)). Unfortunately, due to an experimental error of about 10%, no definite quantitative conclusion about the influence of E_{ad} on θ at constant t_{ad} can be

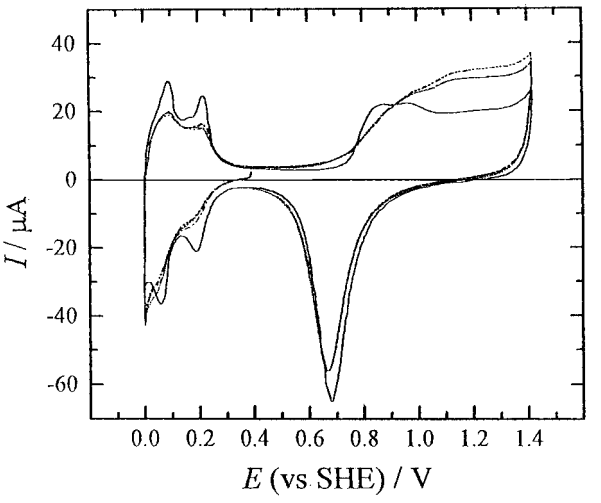

Fig. 8. Voltammograms run at $v = 0.05$ V s^{-1} in 0.5 M sulfuric acid starting from $E = 0.39$ V covering the range 0–1.4 V using platinum electrodes that were previously left in contact with freshly prepared aqueous 0.02% w/v agarose + 0.5 M sulfuric acid, for $t_{ad} = 600$ s at different E_{ad}; $E_{ad} = 0$ V (dot-dashed trace); $E_{ad} = 0.2$ V (dotted trace); $E_{ad} = 0.1$ V (double dot-dashed trace). Full trace corresponds to the blank in aqueous 0.5 M sulfuric acid at 298 K.

drawn. On the other hand, at constant E_{ad}, and 5 s $\leqslant t_{ad} \leqslant$ 4500 s, the following linear θ against log t_{ad} relationship is obeyed (Figure 9(b)):

$$\theta = (-62 \pm 7) + (32 \pm 2) \log t_{ad}/\text{min} \quad (1)$$

as expected for an adsorption process obeying an Elovich-type adsorption equation [20] with a slope in Equation 2 that is independent of E_{ad}.

3.4. *Data from flow cell experiments*

Flow cell data allowed us to distinguish between possible adsorption and electroadsorption processes and detect other faradaic reactions that might be due to the presence of the additive on the electrode surface. These experiments started by recording a cyclic voltammogram of platinum in aqueous 0.5 M sulfuric acid (blank). Subsequently, the current transient at a constant E_{ad} selected in the range 0.080 V $\leqslant E_{ad} \leqslant$ 0.658 V was started and, after approximately 5 min, the acid electrolyte was replaced by admitting flowing freshly prepared aqueous agarose-containing 0.5 M sulfuric acid into the cell. In this case, changes in the current might be due either to electroadsorption or perturbations at the metal–solution interface caused by the flow of the solution and/or the change in charge of the electrical double layer. Afterwards, holding the potential at E_{ad}, the agarose-containing solution was washed out with aqueous 0.5 M sulfuric acid. Finally, in this solution a single voltammogram from E_{ad} to 0.0 V, up to 1.40 V, and reversely to 0.39 V was run, and then cyclic voltammetry was continued until the blank voltammogram was attained (Figure 10). The time required to recover this voltammogram was taken as an indication of the platinum-adsorbate interaction strength.

For the whole range of E_{ad} only small, noisy cathodic current transients were recorded (Figure 10(a)), the charge integrated from these transients being always smaller than 0.09 mC cm^{-2}. This value indicates that either only a small number of molecules are electroadsorbed or, more likely, that a double layer charging difference occurs that can be attributed to the change in the electrical double layer capacitance caused by ad-

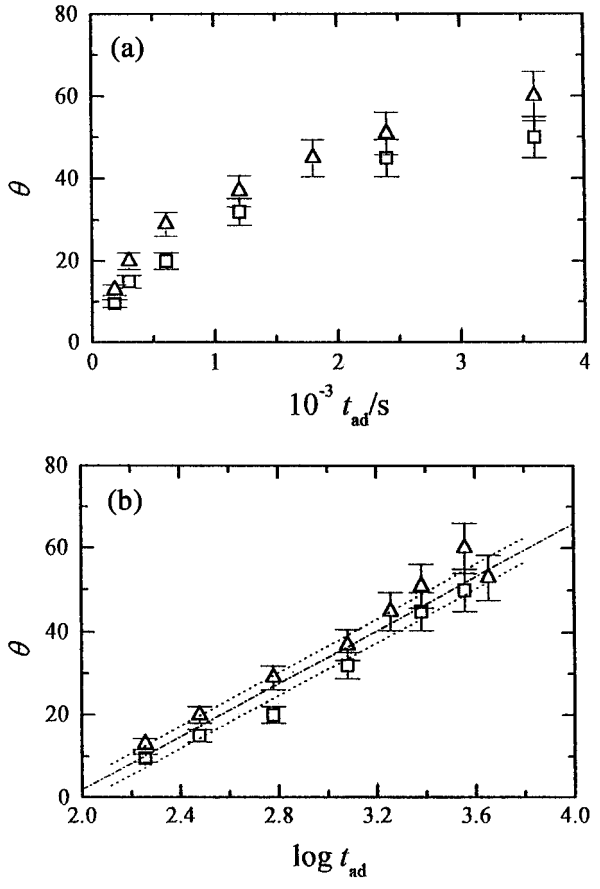

Fig. 9. (a) θ against t_{ad} and (b) θ against log t_{ad} plots. Data from Figure 8. The linear relationship in (b) corresponds to an Elovich-type adsorption equation.

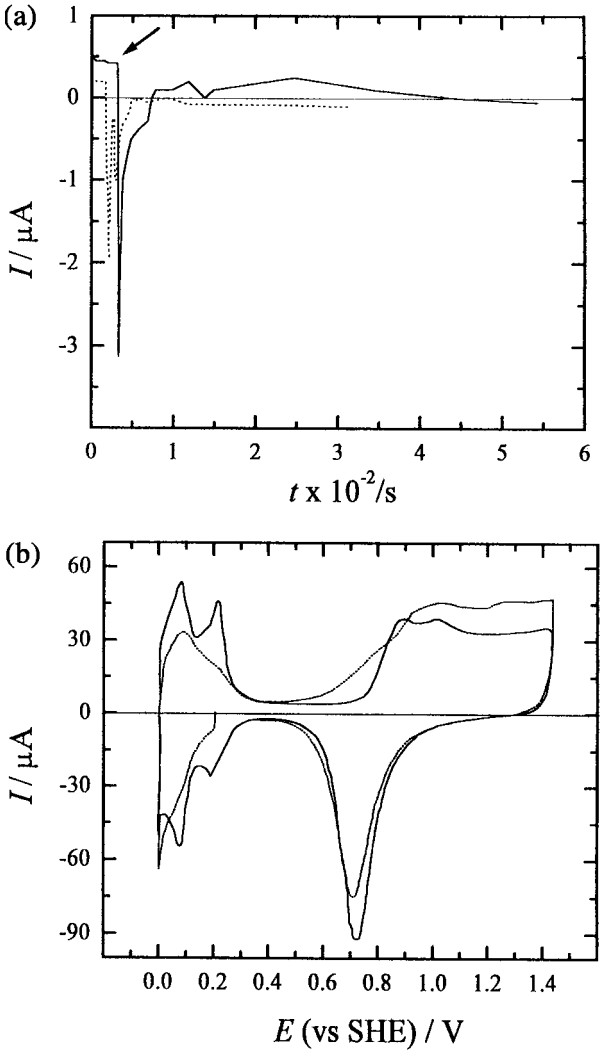

Fig. 10. (a) Transients at $E_{ad} = 0.2$ V. (···) Blank; (—) aqueous 0.02% w/v agarose + 0.5 M sulfuric acid. Arrow indicates the inlet of the agarose-containing solution. (b) Voltammograms of a platinum electrode in 0.5 M sulfuric acid; (···) after previously held at $E_{ad} = 0.2$ V in aqueous 0.02% w/v agarose + 0.5 M sulfuric acid for $t = 660$ s; (—) voltammogram that is similar to that of the blank resulting after cycling at 0.05 V s^{-1} for 40 min.

sorption [13]. Therefore, it seems reasonable to conclude that platinum/aqueous agarose interactions, at least in the range $0.080\ V \leqslant E_{ad} \leqslant 0.658\ V$, are better described as an adsorption rather than an electroadsorption process.

On the other hand, after adsorption the voltammogram shows a decrease in the strongly bound hydrogen adatom charge, and a delay in the initiation of the oxygen-containing layer on platinum (Figure 10(b)). The corresponding electroreduction voltammogram also shows a decrease in the electroreduction charge, indicating a decrease in the degree of surface coverage by oxygen-containing species. Accordingly, adsorbates produced from agarose preferentially inhibit the electrodesorption charge of strongly bound hydrogen atoms on platinum, as is usually found for other organic molecules on the same metal [13]. In contrast to silver, these voltammograms also confirmed that agarose adsorbates are rather strongly bound to platinum as the original voltammogram was hardly recovered after potential cycling between 0 and 1.4 V at $v = 0.05\ V\ s^{-1}$ for several minutes.

3.5. *Viscosity data*

The changes in the rheological behaviour of both free- and agarose-containing electrolyte solutions were determined by comparing the flow time (t_f) of each solution to that of water taken as the reference. For each agarose-containing solution the value of t_f was measured as a function of the solution standing time for a period of four weeks. For each standing period, a series of at least five values of t_f was measured, the first value being taken as the most representative of each particular series.

For aqueous $c_{aga} \leqslant 0.02\%$ w/v + 0.5 M sulfuric acid, the first value of t_f remained almost unchanged after standing the solution for one week, for instance, for $c_{aga} = 0.02\%$ w/s, $t_f = 55$ s. Conversely, for aqueous $c_{aga} \geqslant 0.02\%$ w/v + 0.014 M silver sulfate + 0.5 M sodium sulfate + 0.01 M sulfuric acid, the value of t_f depends on the standing period. Thus, for $c_{aga} = 0.05\%$ w/v, t_f reached a minimum value after standing for two weeks, then increasing slowly (Figure 11). However, it should be noted that for $c_{aga} \geqslant 0.02\%$ w/v, the value of t_f increases in going from the first in the series onwards, presumably because of a significant increase in the percentage of gel structure with c_{aga}. In fact, the relative percentage of free fibres (X_L) calculated for $c_{aga} = 0.05\%$ w/v from the equation [7]

$$X_L = 1 - 0.21\, c_{aga}^{1/2} \tag{2}$$

is 0.95. Then, it is reasonable to conclude that the rheological change of agarose-containing solutions is related to changes in both the composition and the structure of the gel fraction caused by the chemical decomposition of standing agarose-containing solutions.

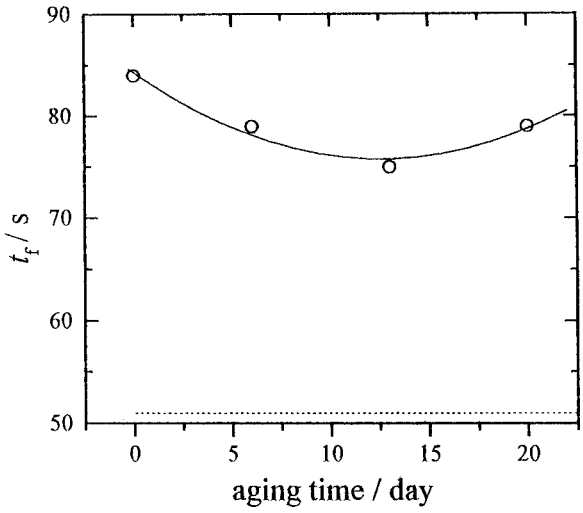

Fig. 11. Typical flowing time against standing time plot for aqueous 0.05% w/v agarose + 0.014 M silver sulfate + 0.5 M sodium sulfate + 0.01 M sulfuric acid under nitrogen saturation at 298 K. Dotted line corresponds to water taken as the reference.

3.6. *Infrared spectra*

The infrared spectrum of a solid sample of agarose, as received, in potassium bromide (Figure 12(a)) shows two broad peaks in the 2500–3700 cm^{-1} region, a small pair of peaks in the 2000–2500 cm^{-1} region and a strong peak at 1650 cm^{-1}, that is, in the spectral region of O—H absorption [21, 22]. The peak at 1650 cm^{-1} can be assigned to the presence of water. The spectrum of dried, gelled agarose that was separated from aqueous sodium sulfate after standing for two weeks (Figure 12(b)) shows a decrease in the intensity ratio of the bands found in the 2500–3700 cm^{-1} region. The changes in these O—H absorption bands are consistent with structural modifications in the gel caused by the standing decomposition of agarose–containing solutions, in agreement with conclusions from the flow time measurements referred to in 3.5.

4. Discussion

4.1. *Phenomenological summary*

The preceding results indicate that the presence of agarose produces changes in the viscosity of the solutions; these changes depending on whether they are freshly prepared or used after a standing period, as well as on the constituents of the solutions. It is known that below a critical concentration of agarose the solution behaves as non-newtonian, whereas above it, it turns into a gel-like structure behaving as a Bingham plastic [7, 23]. From the rheological standpoint, the stability of aqueous agarose-containing sulfuric acid decreases as either c_{aga} or $c_{H_2SO_4}$ is increased. Thus, for aqueous agarose 0.1% w/v + 0.014 M silver sulfate + 0.5 M sodium sulfate + 0.01 M sulfuric acid, after 2.5 h

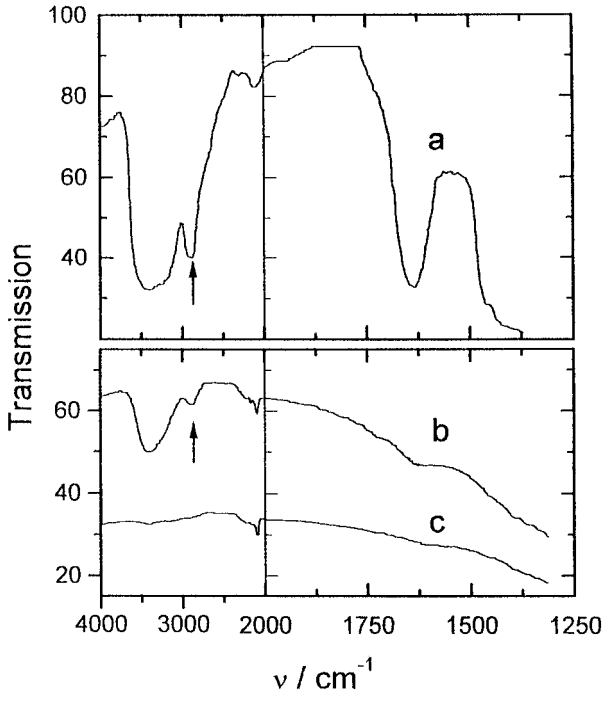

Fig. 12. Infrared spectra in potassium bromide, (a) Pure agarose. (b) Dried, gelled agarose after standing for two weeks in aqueous sodium sulfate. Arrow indicates changes in O–H absorption bands produced by ageing.

standing, the decrease in viscosity amounts to 0.1%, and after 18 h it reaches 1%.

On the other hand, the influence of agarose on the voltammetric features of the metal–solution interface depends on both the nature of the metal and the constituents of the solution, and on the standing period of the solution. For each particular solution, this influence appears to be almost independent of the potential applied to the working electrode, at least the equilibrium potential of the hydrogen electrode up to the threshold potential for the electrooxidation of water. This means that a homogeneous chemical decomposition outlives its usefulness for each particular application. Furthermore, the electrocatalytic properties of platinum become useful to detect products from agarose decomposition.

4.2. *Stability of agarose-containing aqueous solutions and convective mass transport*

Recently, it has been demonstrated [7] that the critical concentration of aqueous agarose related to the sol–gel transition, that is, from a non-newtonian to Bingham plastic fluid, is $c^*_{aga} = 0.12\%$ w/v, a value that coincides with the critical concentration of agarose required to form a percolation structure that prevents convective fluid motion. The magnitude of this effect, which is of importance for the interpretation of kinetic data in heterogeneous reactions, can be estimated from the Grashof number (*Gr*) that indicates the buoyancy to viscous force ratio *Gr* is defined as [24]

$$Gr = \alpha' g L^3 / \nu^2 \tag{3}$$

where $\alpha' = (c_0/\rho)(\partial\rho/\partial c)$ is the densification coefficient, c_0 being the concentration of the reacting species in the bulk solution, ρ and ν are the density and kinematic viscosity of the solution, g is the acceleration due to gravity, and L is the characteristic length of the system. Here, L is the height of the vertical plate working electrode for $L \ll$ anode-cathode distance, and for percolated gels L is related to the pore size. For these gels, the effective pore size radius (P_E) is a power function of the concentration of agarose [25–27] of the form

$$P_E = 114\, c_{aga}^{-1.12} \tag{4}$$

Therefore, for sols taking $\nu = 1.6 \times 10^{-2}$ cm^2 s^{-1}, $L = 0.05$ cm, $g = 980$ cm s^{-2}, and $\alpha' = 0.004$ [8], this results in $Gr(\text{sol}) \simeq 0.03$, while for gelled solution with $c_{aga} = 0.3\%$ w/v and 300 nm $\leqslant L \leqslant$ 1000 nm, $Gr(\text{gel}) \simeq 10^{-9}$–$10^{-10}$. The choice of different values of L for sols and gels can be justify because of the change in the mass transport mechanism. For sols covective mass transport is pinning-free and principally depends on cell design, whereas for gelled solutions the reverse situation arises. In this case, diffusion through pores becomes the dominant mass transport mechanism because of the influence of pinning [8]. Therefore, for gelled solutions mass transport is due almost exclusively to pure diffusion.

On the other hand, the usefulness of these solutions depends on their stability. The changes in t_f in aqueous 0.05% w/v agarose + 0.014 M silver sulfate + 0.5 M sodium sulfate + 0.01 M sulfuric acid sol (Figure 11) indicates the range of time in which this solution is appropriate to follow up the influence of viscosity on physico-chemical phenomena. Likewise, from Figure 4, it can be concluded that, for sulfuric acid concentrations lower than about 0.01 M and in the presence of a relatively large concentration of inert electrolyte, sols remain stable for a much longer time.

4.3. *Chemical reactions in the colloidal state*

Data from viscosity and infrared spectroscopy provide information about dominant intramolecular interactions. For agarose, which contains a few donor OH groups per molecule, changes in the O—H stretching bands spectra are observed (Figures 12(a) and (b)). For polysaccharides the O—H stretching bands are usually broad and centred at 3320–3340 cm^{-1} [21], but for intramolecularly bonded hydroxyls in dynamic equilibrium with solvent-bonded species these bands can be observed in the 3250–3270 cm^{-1} region, as recorded. Furthermore, the hydrogen-bonded patterns of unsubstituted polysaccharides in the solid state produce

complex O—H absorption bands in the 3200–3600 cm^{-1} region, although in this case, the contribution of individual hydrogen is usually difficult to evaluate because of the additional complications introduced by water absorption [22].

In agarose, as in other polysaccharides, the repeating sequence structure is interrupted by the occurrence of other residues [21]. Such interruptions can produce a remarkable modification in bulk properties by terminating intermolecular association through structurally regular junction zones leading to a 3D network, including island formation. The same effect is also produced by departure from the regular primary sequence [6, 21]. The interchain association through double helical junction zones is terminated by galactose residues in the normal, unbridged ring form in place of the fused anhydride ring structure. This introduces a backbone kink that cannot be accommodated within the ordered structure [6, 21]. The formation of this molecular organization, in particular intermolecular networks, has been proved by rheological studies of agarose sols and gels [7]. These structural changes are consistent with the infrared spectral features mentioned above.

On the other hand, it is known that the homogeneous hydrolysis of cellulosic materials is favoured at high concentrations of sulfuric acid [6]. Among possible products from the acidic hydrolysis of agarose are lower molecular weight polysaccharides as well as other organic residues with a higher percentage of carbon. The kinetics of the decomposition reaction can be expressed by the first order rate equation,

$$N = N_0 \exp(-kt) \tag{5}$$

where N is the number of chain links in the adsorbed molecule, and N_0 corresponds to the value of N for $t = 0$. The value of N_0 is proportional to the initial concentration of reactant. For $c_{aga} = 0.02\%$ w/v and $c_{H_2SO_4} = 0.5$ M, at 298 K, the value of the rate constant is $k = 7.2 \times 10^{-5}$ s^{-1} [6]. This value corresponds to a half-life time $t_{1/2} = 1.4 \times 10^4$ s.

In principle, decomposition products should contribute to a decrease in t_f but as shown in Figure 11, after reaching its minimum value, t_f begins to increase steadily. This suggests that new interactions among hydrolysis products and remaining agarose chains alter the configuration and the fraction of the colloid network structure in the system. Therefore, compensating effects, probably related to the formation of various decomposition products and intermediates from agarose, might be responsible for the viscosity behaviour.

4.4. *Colloidal solution–metal surface interaction*

There are remarkable differences between voltammetric runs from agarose-containing solutions using silver and platinum (Figures 5 and 6). In the former case, the changes in the lead upd/anodic stripping voltammogram caused by the presence of agarose mainly appear in the anodic and cathodic current peak multiplicity (Figure 5). Thus, the blank voltammogram shows the pair of peaks Ia–Ic, IIa–IIc, and IIIa–IIIc that are assigned to the contribution of Ag (1 1 1) crystal faces [16–18], whereas in the presence of agarose ($c_{aga} = 0.02\%$ w/v) the height of these peaks is largely engulfed in poorly defined, broad voltammetric peaks, irrespective of t_{ad}. In contrast, the overall voltammetric anodic and cathodic charge densities, both in the blank and in the agarose-containing solution, become approximately the same, their ratio being close to one. Hence, from these data it can be concluded that agarose modifies the orderly structure of the initial silver surface. In fact, it is known that the surface mobility of silver atoms is enhanced by the presence of a fractional lead atom monolayer [15–17]. Our results suggest that agarose chains at the metal–solution interface also interfere with the surface diffusion of metal atoms on the electrode surface. This is an additional contribution that has to be considered to explain why the growth mode of silver electrodeposits is modified by the presence of agarose in the plating solution [8].

The voltammetric behaviour of fresh and standing agarose sols on platinum indicates the presence of at least two kinds of decomposition product that are associated with the different times required for the inhibition of the hydrogen atom electrosorption processes in fresh and standing solutions (Figures 6 and 7). In fact, the faster this inhibition effect the longer the standing period of aqueous agarose-containing 0.5 M sulfuric acid. It should be noted that 3,6-anhidro galactose residues from agarose probably can also be depolymerized in the acid solution [6].

Voltammetric results on platinum confirm that adsorbate formation from agarose does not depend primarily on E_{ad}, at least for values in the range between the hydrogen adatom region up to the threshold potential for the electroadsorption of OH species from water. However, platinum–agarose interaction for fresh sols, and platinum–agarose decomposition product interaction for standing sols yield adsorbed residues that exhibit voltammetric electrooxidation features as those recorded from simpler organic molecules. Accordingly, the voltammetric response of platinum should be related to the presence of adsorbates principally resulting from the chemical decomposition of agarose in the acid solution.

The voltammetric electrooxidation of adsorbates formed on platinum is characterized by three anodic current peaks at 0.55 V (peak I) , 0.85 V (peak II) and 1.175 V (peak III) (Figures 6 and 7). Peak I appears in the potential range where simpler organic molecules containing —CO and —COOH groups, including 'reduced carbon dioxide' residues [30–37] are electrooxidized. Conversely, peaks II and III are found in the range where OH— and oxygen-adsorbed species are formed on platinum from the electrooxidation of water, both competing with the adsorption of sulphate anions

for bare platinum surface sites [28, 29]. Therefore, peaks I and II are related to the electrooxidation of weakly and strongly bonded adsorbates from agarose decomposition. In these cases, the electrooxidation occurs via the open chain of the aldehyde forms [31, 33].

Kinetic data for agarose decomposition in aqueous 0.5 M sulfuric acid can be estimated from $(q_a)_{ad}$, the charge of the peak III, which corresponds to the largest electrooxidation charge of strongly bonded surface residues, and $(q_a)_H$, the residual hydrogen atom electrooxidation charge in agarose containing acid solution. Considering that the ratio $(q_a)_{ad}/(q_a)_H = \Gamma$ is proportional to N, the number of chain links at the adsorbed molecule, the plot of log Γ against t_{ad} (Figure 13) fits a reasonable straight line as expected for a first order process. The rate constant calculated from the slope of the straight line is $k = 4.3 \times 10^{-3}$ min^{-1}, and $t_{1/2} = 2.3 \times 10^2$ min $\simeq 1.4 \times 10^4$ s. This value, within experimental scatter, coincides with those for other polysaccharides [6, 37].

The voltammetric behaviour of adsorbates formed from agarose decomposition products also agree with the conclusions of earlier studies about saccharide electrooxidation [34–38]. Accordingly, for molecules involving a hemiacetalic group such as xylose and arabinose, two main reaction stages can be distinguished, the first being the electroadsorption of molecules involving the electrooxidation of the hydrogen atom in the C-l atom that is the most labile, and the second to the strongly bonded residue. Therefore, the complex overall mechanism, which has already been discussed extensively for the electrooxidation of glucose and other related compounds [41–43], can be extended to the electrochemical behaviour of agarose residues formed on platinum in acid solution. Furthermore, the good coincidence of rate constants for the decomposition of different polysaccharides is consistent with hydrolysis mechanisms involving the rupture of glycosidic bonds. This would imply that all linkages behave alike in the overall process [38, 40].

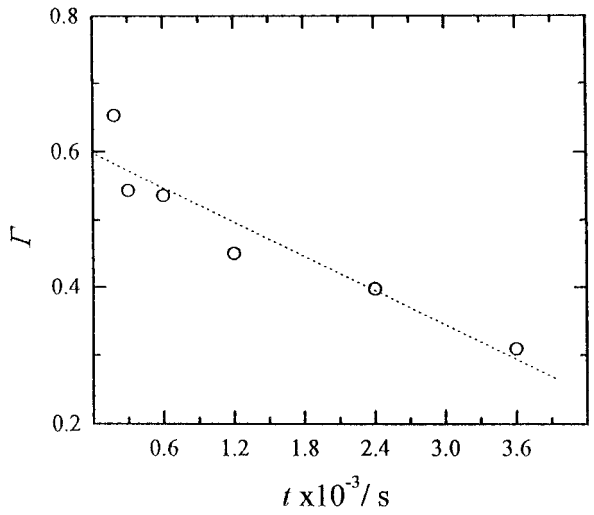

Fig. 13. Log Γ against t_{ad} plot. Data for the rate of agarose decomposition resulting from the electrooxidation voltammogram of residues adsorbed on platinum from aqueous agarose + 0.5 M sulfuric acid; 298 K.

5. Conclusions

The stability of aqueous agarose solutions decreases as the concentration of sulphuric acid is increased. This fact is reflected in changes of the flow times of the solution, the open circuit potential of a platinum electrode in those solutions, and the appearance of decomposition products that are detected electrochemically.

Viscosity data and infrared spectra show that intra- and intermolecular interactions involving hydrogen bonding depend on the agarose concentration and ionic composition, including pH. These interactions play a key role in the sol–gel transition and on the extent and size distribution of gelled domains. The morphology of silver electrodeposits depends on the sol and gel structure.

The reversible potential of the silver/aqueous silver ion electrode in 0.014 M silver sulfate + 0.5 M sodium sulfate + 0.01 M sulfuric acid remains unchanged over several weeks, irrespective of the addition of agarose. However, the presence of agarose modifies the voltammetric features of lead upd/anodic stripping from silver by influencing the peak multiplicity, although the overall voltammetric charge remains almost the same over several hours. In this case, agarose–silver adsorption phenomena produce a change in the distribution of surface site energy without an appreciable surface blockage.

The interaction of agarose and products resulting from its chemical decomposition leads to adsorbates that inhibit hydrogen atom electrosorption on platinum. The greater inhibition capability is due to agarose decomposition products. Adsorbate formation follows an Elovich-type equation. The voltammetric electrooxidation characteristics of these adsorbates are similar to those of adsorbates produced from simpler saccharides on platinum. The time dependence of the voltammetric charge balance, based upon the adsorbate electrooxidation charge and the decrease in the hydrogen electroadsorption charge, follows first order kinetics with a rate constant that is of the same order as those found for the chemical decomposition of other polysaccharides. This is consistent with hydrolysis mechanisms involving the rupture of glycosidic bonds.

The results establish conditions for the application of agarose to the study of the influence of gelling, particularly for those processes yielding new solid phases.

Acknowledgements

This work was financially supported by PICT-98 06-03251 from Agencia Nacional de Promoción Científica y

Técnológica (Argentina). AEB is a Member of the Research Career of the Comisión de Investigaciones Científicas de la Provincia de Buenos Aires. MAP acknowledges Consejo Nacional de Investigaciones Científicas y Técnicas for the fellowship granted.

References

1. A.J. Arvia, J.C. Bazán and J.S.W. Carrozza, *Electrochim. Acta* **13** (1968) 81.
2. M. Wang, Nai-ben Ming and P. Bennema, *Phys. Rev. E* **48** (1993) 3825.
3. P. Carro, A. Hernández Creus, S. González, R.C. Salvarezza and A.J. Arvia, *J. Electroanal. Chem.* **310** (1991) 361.
4. P. Carro, S.L. Marchiano, A. Hernández Creus, S. González, R.C. Salvarezza and A.J. Arvia, *Phys. Rev. E* **48** (1993) R2374.
5. P. Carro, S. Ambrosolio, S.L. Marchiano, A. Hernández Creus, R.C. Salvarezza and A.J. Arvia, *J. Electroanal. Chem.* **396** (1995) 183.
6. D.A. Rees, E.D. Morris, D. Thom and J.K. Madden, *in* G.O. Aspinall (Ed.), 'The Polysaccharides', Vol. I (Academic Press, New York, 1982), Chapter 5, p. 195.
7. J.M. García Ruiz, M.L. Novella, R. Moreno and J.A. Gavira, *J. Crystal Growth* **232** (2001) 165.
8. M.A. Pasquale, S.L. Marchiano and A.J. Arvia, to be submitted.
9. S. Arnott, A. Fulmer and W.E. Scott, *J. Mol. Biol.* **90** (1974) 269.
10. D.A. Rees and E.J. Welsh, *Angew. Chem. Int. Eng. Edition* **16** (1977) 214.
11. M.C. Arévalo, E. Pastor, S. González, A. Arévalo, M.C. Giordano and A.J. Arvia, *J. Electroanal. Chem.* **281** (1990) 245.
12. E. Pastor, M.C. Arévalo, S. González and A.J. Arvia, *Electrochim. Acta* **36** (1991) 2003.
13. B. Damaskin, O.A. Petrii and B.B. Batrakov, 'Adsorption of Organic Compounds on Electrodes' (Plenum Press, New York, 1971).
14. A. Bewick and B. Thomas, *J. Electroanal. Chem.* **84** (1977) 127.
15. A.H. Bort, K. Juettner, W.J. Lorenz and E. Schmidt, *J. Electroanal. Chem.* **90** (1978) 413.
16. K. Juettner, *Electrochim. Acta* **31** (1986) 917.
17. E. Schmidt and H. Siegenthaler, *J. Electroanal. Chem.* **150** (1983) 59.
18. A. Popov, N. Dimitrov, O. Velev, I. Vitanov, E. Budewski, E. Schmidt and H. Siegenthaler, *Electrochim. Acta* **34** (1989) 265.
19. A.A. Hernández Creus, P. Carro, S. González, R.C. Salvarezza and A.J. Arvia, *J. Electrochem. Soc.* **142** (1995) 3806.
20. A.W. Adamson, 'Physical Chemistry of Surfaces' (J. Wiley & Sons, New York, 1982).
21. A.S. Perlin and B. Casu, *in* G.O. Aspinall (Ed.), 'The Polysaccharides', Vol. I (Academic Press, New York, 1982), Chapter 4, p. 182.
22. B. Casu, M. Reggiani, G.G. Gallo and A. Vigevani, *Tetrahedron* **22** (1966) 3061.
23. R.N. Weltmann, *in* F.R. Eirich (Ed.), 'Rheology, Theory and Applications' (Academic Press, New York, 1972), Chapter 6, p. 193.
24. V.E. Levich, 'Physicochemical Hydrodynamics' (Prentice Hall, Englewood Cliffs, NJ, 1962).
25. P.G. Righetti, B.C.W. Frost and S.R. Snyder, *Biochem. Biophys. Methods* **4** (1981) 347.
26. A.G. Ogstron, *J. Chem. Soc. Faraday Trans.* **54** (1985) 1754.
27. G.A. Griess, E.T. Moreno, R.A. Easoni and P. Serwer, *Biopolymers* **28** (1989) 1475.
28. N.R. de Tacconi, J.O. Zerbino, M. Folquer and A.J. Arvia, *J. Electroanal. Chem.* **85** (1977) 213.
29. C. Pallotta, N.R. De Tacconi and A.J. Arvia, *Electrochim. Acta* **26** (1981) 261.
30. K. Ito, S. Ikeda, H. Yamaguchi, K. Ito and T. Kondo, *Denki Kagaku* **43** (1978) 141.
31. H. Lerner, J. Giner, J. Soeldner and C. Colton, *J. Electrochem. Soc.* **126** (1979) 237.
32. A.E.M. Skour, *Electrochim. Acta* **22** (1977) 313.
33. J.J. Christensen, J. Howard Rytting and R.M. Izett, *J. Chem. Soc. London B* (1970) 1646.
34. M.L.B. Rao and R.F. Drake, *J. Electrochem. Soc.* **116** (1969) 334.
35. S. Ernst, J. Heitbaum and C. Hamann, *J. Electroanal. Chem.* **100** (1979) 173.
36. S. Ernst, J. Heitbaum and C. Hamann, *Ber. Bunsenges. Phys. Chem.* **84** (1980) 50.
37. M.F.L. de Mele, H.A. Videla and A.J. Arvia, *J. Electrochem. Soc.* **129** (1982) 2207.
38. M.F.L. de Mele, H.A. Videla and A.J. Arvia, *Bioelectrochem. Bioenerg.* **9** (1982) 469.
39. R.H. Marchessault and P.R. Sundararajan, *in* G.O. Aspinall (Ed.), 'The Polysaccharides', Vol. II (Academic Press, New York, 1982), Chapter 1, p. 24.
40. G.O. Aspinall, *in* G.O. Aspinall, (Ed.), 'The Polysaccharides', Vol. I (Academic Press, New York, 1982), Chapter 1, p. 56.
41. P. Ballinger and F.A. Long, *J. Am. Chem. Soc.* **82** (1960) 795.
42. J.J. Christensen, J. Howard Rytting and R.M. Izett, *J. Chem. Soc. London B* (1970) 1646.
43. A.M. Castro Luna, A.E. Bolzan, M.F.L. de Mele and A.J. Arvia, *Pure Appl. Chem.* **63** (1991) 1599.